

COMMUNICATIONS

Correlation of Isotropic Shifts and Chemical Shift Anisotropies by Two-Dimensional Fourier-Transform Magic-Angle Hopping NMR Spectroscopy

AD BAX, NIKOLAUS M. SZEVERENYI, AND GARY E. MACIEL*

Department of Chemistry, Colorado State University, Fort Collins, Colorado 80523

Received November 29, 1982

During the 1960s Andrew and others examined the rapid spinning of a sample about an axis that makes an angle of $54^{\circ} 44'$ with the direction of the static magnetic field (H_0) in order to remove broadening effects in the NMR spectra of solids (1-3). It was much later when Schaefer and Stejskal (4) applied this approach, magic-angle spinning (MAS), to remove broadening due to chemical shift anisotropy (CSA) in ^{13}C NMR, combining this approach with high-power ^1H decoupling and cross polarization (CP). The resulting levels of resolution and sensitivity obtained with this combination have made the ^{13}C CP-MAS experiment the most widely applied solid state NMR experiment in recent years.

As powerful, versatile, and popular as the ^{13}C CP-MAS experiment has become, there remain some characteristics that limit its usefulness in certain types of applications. Technological problems persist in techniques for spinning the sample rapidly, problems that are intensified by the scaling of CSA with increasing magnitude of the static field (H_0), although recent advances show great promise for alleviating these problems (5, 6). Another limitation of the usual CP-MAS ^{13}C experiment is that it eliminates the potentially useful information embodied in the CSA pattern, i.e., independent values of the three principal elements of the shielding tensor, σ_{11} , σ_{22} , and σ_{33} . Only the trace, actually $(\sigma_{11} + \sigma_{22} + \sigma_{33})/3$, of the shielding tensor survives under MAS. Techniques have been proposed for retrieving CSA information from a MAS experiment (7-11); although each of these techniques has merits, each suffers from disadvantages.

Introduced here is a two-dimensional (2-D) Fourier transform (FT) technique which presents the isotropic average chemical shift, $\sigma_i = (\sigma_{11} + \sigma_{22} + \sigma_{33})/3$, in one frequency dimension (F_1) and the static CSA powder pattern along the other frequency axis (F_2). The experiment is carried out using discrete "hops" between evolution segments, rather than continuous sample spinning, and no spinning sidebands are produced. As the detection occurs on a static sample, the signal decays more rapidly than in a normal MAS experiment, and sensitivity suffers correspondingly. Nevertheless, the experiment shows considerable promise, not only for the CSA results it is capable of

* To whom correspondence should be addressed.

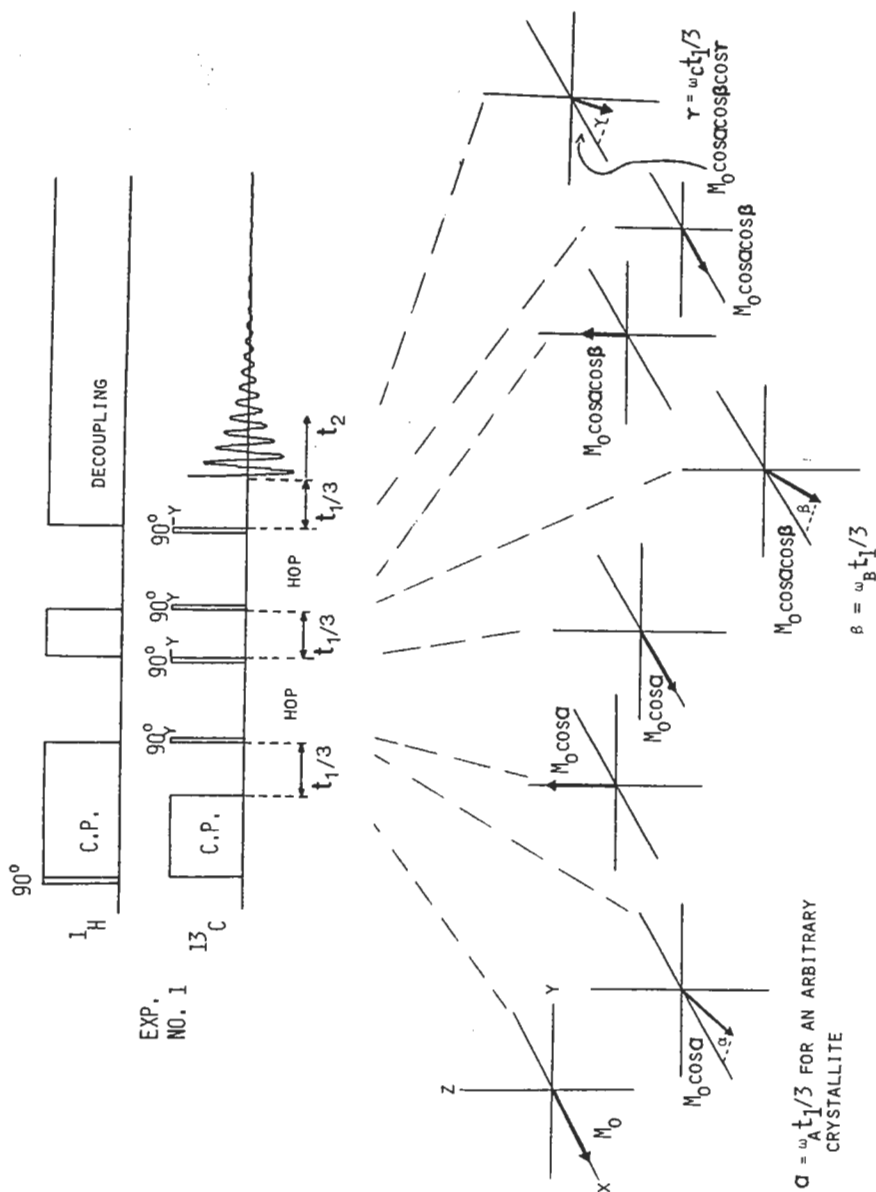


FIG. 1. Pulse sequence for one of the four steps of the magic-angle hopping experiment and the evolution of the ^{13}C magnetization during this sequence. During the time intervals indicated with "hop" the sample is rotated by 120° about the magic-angle axis. During the "hop" period, proton decoupling is switched off, and transverse magnetization defocuses rapidly. The results of three similar experiments with the different ^{13}C rf phases given in Table I are combined as described in the text.

providing in its present form for which it can serve as a

The experiments were carried out employing a Nicolet 1180 spectrometer operating at 2.3 T. The probe (about 1.5 cm^3 volume) is rotated in 120° jumps about an axis executed in about 150 ms, at the top of the probe and magnet arrangement. The ^{13}C rf field

A simple form of the magnetization vector is shown in Fig. 1. The experiment is performed by a $t_1/3$ evolution period in an arbitrary crystallite in which the transverse ^{13}C magnetization is stored along z by a 90° pulse. The sample is quickly rotated to proceed under the new orientation. In the next diagram, after a similar sequence at resonance frequency ω_C , the magnetization after a $t_1/3$ period is $M_0 \cos \alpha \cos \beta$ when data acquisition in the xz plane is performed according to ω_C , the magnetization is $M_0 \cos \alpha \cos \beta \exp(i\omega_C t_1/3)$.

Three similar experiments are performed only in the combinations specified, the ^{13}C xy magnetization

$$M_1(t_1) =$$

$$M_2(t_1) =$$

$$M_3(t_1) =$$

$$M_4(t_1) =$$

The sum of these four magnetization vectors

$$M_{\Sigma}(t_1) =$$

$$=$$

For this case, in which $\omega_C = \omega$, the three orientations related to the magic angle can be shown (7, 10), and it corresponds to the trace of the

providing in its present form, but also for the class of new types of future experiments for which it can serve as a prototype.

The experiments were carried out at 25.0 MHz (^{13}C) on a home-built spectrometer, employing a Nicolet 1180 data system and a wide-bore 3.7 T Nalorac magnet operating at 2.3 T. The probe contains a mechanical device for rotating the sample (about 1.5 cm³ volume) in a Kel-F cylinder of 1.1 cm inside diameter) in discrete 120° jumps about an axis oriented at the magic angle relative to \mathbf{H}_0 . Each jump is executed in about 150 ms, driven by a computer-controlled stepping motor mounted at the top of the probe and coupled to the sample by a suitable connecting-rod/gear arrangement. The ^{13}C rf field was 48 G and the ^1H field 12 G.

A simple form of the magic-angle hopping experiment is shown in the diagrams of Fig. 1. The experiment begins with a conventional CP sequence. This is followed by a $t_1/3$ evolution period during which the ^{13}C resonance frequency of a given carbon in an arbitrary crystallite in the static powder is ω_A . After $t_1/3$ the x component of transverse ^{13}C magnetization is $M_0 \cos \alpha$, where $\alpha = \omega_A t_1/3$. This component is then stored along z by a 90_y° pulse. At this point the ^1H decoupler is turned off and the sample is quickly rotated by 120° about the magic-angle axis. A 90_z° pulse brings the stored z magnetization back along x , where evolution for a time $t_1/3$ is allowed to proceed under the new ^{13}C resonance frequency, ω_B . As shown in the vector diagram, after a similar sequence of events involving evolution under a third resonance frequency ω_C , the x component of ^{13}C magnetization at the end of the third $t_1/3$ period is $M_0 \cos \alpha \cos \beta \cos \gamma$ (where $\beta = \omega_B t_1/3$, $\gamma = \omega_C t_1/3$). At this point, when data acquisition in the t_2 domain begins under evolution of the ^{13}C magnetization according to ω_C , the total xy magnetization, $M_1(t_1)$, can be represented as $M_0 \cos \alpha \cos \beta \exp(i\omega_C t_1/3)$.

Three similar experiments are carried out which differ from the one shown in Fig. 1 only in the combinations of rf phases employed in the 90° ^{13}C pulses. These combinations are summarized in Table 1. For the four hopping experiments thereby specified, the ^{13}C xy magnetizations at the beginning of the t_2 period are

$$M_1(t_1) = M_0 \cos(\omega_A t_1/3) \cos(\omega_B t_1/3) \exp(i\omega_C t_1/3)$$

$$M_2(t_1) = iM_0 \sin(\omega_A t_1/3) \cos(\omega_B t_1/3) \exp(i\omega_C t_1/3)$$

$$M_3(t_1) = iM_0 \cos(\omega_A t_1/3) \sin(\omega_B t_1/3) \exp(i\omega_C t_1/3)$$

$$M_4(t_1) = -M_0 \sin(\omega_A t_1/3) \sin(\omega_B t_1/3) \exp(i\omega_C t_1/3).$$

The sum of these four $M(t_1)$ values is

$$\begin{aligned} M_\Sigma(t_1) &= M_0 \exp(i\omega_A t_1/3) \exp(i\omega_B t_1/3) \exp(i\omega_C t_1/3) \\ &= M_0 \exp(i\{\omega_A + \omega_B + \omega_C\}t_1/3). \end{aligned} \quad [1]$$

For this case, in which ω_A , ω_B , and ω_C correspond to chemical shifts of a crystal at three orientations related to each other by 120° rotations about a magic-angle axis, it can be shown (7, 10, 11) that the sum in brackets on the right side of Eq. [1] corresponds to the trace of the chemical tensor ($\text{Tr } \sigma = \sigma_{11} + \sigma_{22} + \sigma_{33}$). Hence

$$M_\Sigma(t_1) = M_0 \exp(i\omega t) \quad [2]$$

TABLE 1
PHASES OF THE ^{13}C rf PULSES AND OF THE RECEIVER IN THE SEQUENCE OF FIG. 1

Experiment no.	CP segment ^a	Hopping segment ^b				Acquisition ^c
		ϕ_1	ϕ_2	ϕ_3	ϕ_4	
1	x	y	-y	y	-y	+
2	x	-x	-y	y	x	+
3	x	y	-y	x	x	-
4	x	-x	-y	-x	-y	-

^a Phase of the ^{13}C pulse in the CP segment.

^b Phases of the rf in the four 90° ^{13}C pulses in the sequence of Fig. 1.

^c Phase of the ^{13}C receiver during data acquisition.

where ω_i is the resonance frequency corresponding to the isotropic shielding, $(\text{Tr } \sigma)/3$.

Taking this ω_i modulation of the ^{13}C magnetization at the beginning of the t_2 period into account, the time dependence of M_z during data acquisition can be written

$$M_z(t_1, t_2) = M_0 \exp(i\omega_i t_1) \exp(i\omega_c t_2) \exp(-[t_1 + t_2]/T_2) \quad [3]$$

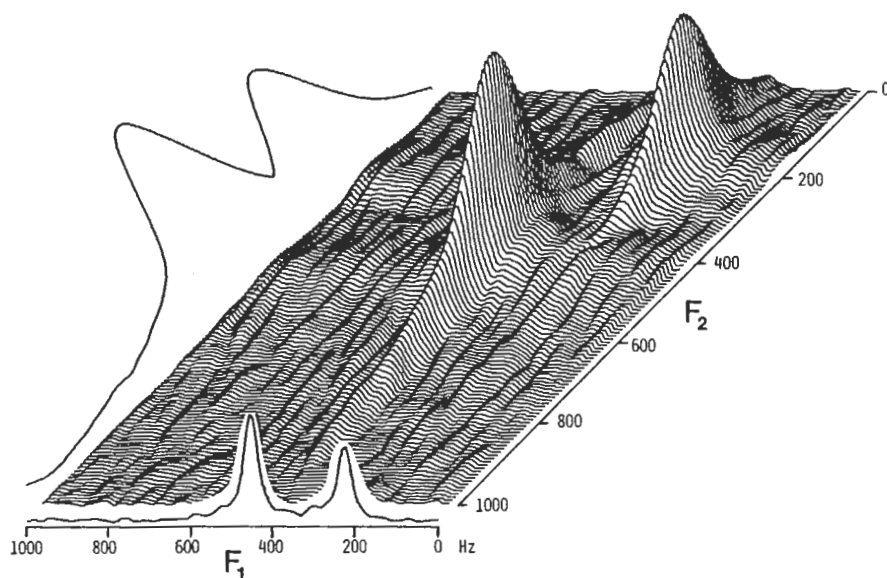


FIG. 2. Two-dimensional magic-angle hopping ^{13}C spectrum of adamantane in the absolute-value-mode presentation, plus the projections of this absolute-value-mode spectrum on both the F_1 and F_2 axes. Four acquisitions were performed per t_1 value with a delay time between experiments equal to 3 sec, and 64 values of t_1 were used. The t_1 increment was equal to 1 msec. The total measuring time was approximately 15 min.

FIG. 3. Magic-angle hopping ^{13}C absolute-value-mode two-dimensional spectra through the two-dimensional spectral shifts. The two proton-bearing responding powder patterns are performed for each value of t_1 , and t_1 were used. The t_1 increment was

where the term in T_2 accounting has been neglected. It is negligible during the hopping. The evolution of the transverse magnetization in the t_2 dimension powder pattern is manifested as modulation at ω_i , yields the

Figure 2 shows the 2-D spectrum shown in Fig. 1. Figure 3 shows the F_1 (horizontal axis) shows the F_2 (vertical axis) show the

These preliminary results of individual peaks of compound approach would yield only one. This and related experiments

The authors are grateful for support from the Colorado State University

1. E. R. ANDREW, A. BRADBECK
2. E. R. ANDREW, *Phil. Trans.*

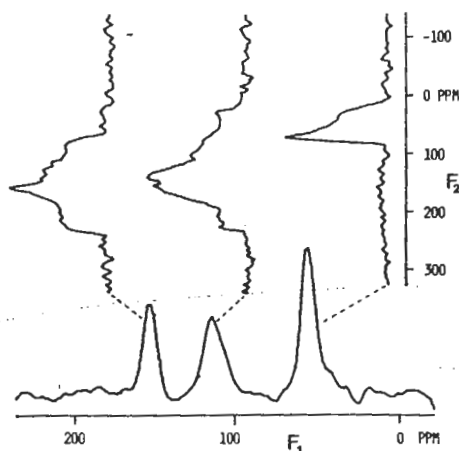


FIG. 3. Magic-angle hopping ^{13}C spectrum of *p*-dimethoxybenzene obtained from a projection of the absolute-value-mode two-dimensional spectrum onto the F_1 axis, and the absorption-mode cross sections through the two-dimensional spectrum showing the static powder patterns for the different ^{13}C chemical shifts. The two proton-bearing aromatic-carbon signals are not resolved in this experiment and the corresponding powder patterns are overlapping in the cross section shown. Six hundred acquisitions were performed for each value of t_1 , with a delay time between experiments equal to 3.5 sec, and 24 values of t_1 were used. The t_1 increment was equal to 75 μsec . The total measuring time was approximately 16 hr.

where the term in T_2 accounts for transverse relaxation and ^{13}C - ^{13}C dipolar broadening has been neglected. Further, it has been assumed that ^{13}C spin-lattice relaxation is negligible during the hopping periods. The factor $\exp(i\omega_c t_2)$ in Eq. [3] describes the evolution of the transverse ^{13}C magnetization of the static sample. Hence, Fourier transformation in the t_2 domain yields a frequency domain (F_2) in which the CSA powder pattern is manifested. Fourier transformation in the t_1 domain, which carries modulation at ω_i , yields the isotropic chemical shift in the F_1 domain.

Figure 2 shows the 2-D FT spectrum obtained on adamantane, using the sequence shown in Fig. 1. Figure 3 shows results on *p*-dimethoxybenzene. The projection along F_1 (horizontal axis) shows the isotropic shift spectrum. The cross sections parallel to F_2 (vertical axis) show the chemical shift anisotropy patterns for the various ^{13}C sites.

These preliminary results show the promise for obtaining powder patterns for individual peaks of complex molecules for which a straightforward nonspinning approach would yield only broad bands of inextricably overlapping powder patterns. This and related experiments are under extensive study.

ACKNOWLEDGMENTS

The authors are grateful for partial support of this research by grants from the U.S. Geological Survey and the Colorado State University Experiment Station.

REFERENCES

1. E. R. ANDREW, A. BRADBURY, AND R. G. EADES, *Nature (London)* **182**, 1659 (1958).
2. E. R. ANDREW, *Phil. Trans. R. Soc. London Ser. A* **299**, 505 (1981).

3. I. J. LOWE, *Phys. Rev. Lett.* **2**, 285 (1959).
4. J. SCHAEFER AND E. O. STEJAKAL, *J. Am. Chem. Soc.* **95**, 1031 (1976).
5. W. T. DIXON, *J. Magn. Reson.* **44**, 226 (1981).
6. W. T. DIXON, *J. Chem. Phys.* **77**, 1800 (1982).
7. M. M. MARICQ AND J. S. WAUGH, *J. Chem. Phys.* **70**, 3300 (1979).
8. E. LIPPMAA, M. ALLA, AND T. TUHESR, "Proceedings of the 19th Congress Ampere, Heidelberg, 1976," p. 113.
9. W. P. AUE, D. J. RUBEN, AND R. G. GRIFFIN, *J. Magn. Reson.* **43**, 472 (1981).
10. Y. YARIM-AGAEV, P. N. TUTUNJIAN, AND J. S. WAUGH, *J. Magn. Reson.* **47**, 51 (1982).
11. A. BAX, N. M. SZEVERENYI, AND G. E. MACIEL, *J. Magn. Reson.*, in press.

Selective Solvent Pulse: Its App

Faculty of Science, Biophy

Strong peaks arising from
for NMR spectroscopists.
when low concentrations
the detection of the weak
HDO peak poses a severe
reduction of signals arising
of interest in the spectrum

Many techniques have
line from the spectrum, or
form) method (1, 2). The
comprehensive descriptive
erature (1, 2). Important
longitudinal relaxation time
than the relaxation time
fulfilled in the case of sm
conditions.

The self-complementary
ample of the latter difficulty
structure at ambient temp
compound in D₂O at 25°C
is by far the most intense
degassed, the longitudinal
appears to be similar to th
from the normal WEFT sp
most of the solute signals a

This situation is remedie
Morris and Freeman (3): i
applied to the residual HD
called DANTE pulse sequen
after a delay time t , at which
a nonselective observation p
DASWEFT (DANTE pulse t
pulse sequence is depicted in